TISSUE ENGINEERING: Part A
Volume 25, Numbers 5 and 6, 2019
© Mary Ann Liebert, Inc.
DOI: 10.1089/ten.tea.2018.0160

termis
Tissue Engineering
& Regenerative Medicine
International Society

ORIGINAL ARTICLE

Partial Meniscus Replacement with a Collagen-Hyaluronan Infused Three-Dimensional Printed Polymeric Scaffold

Salim A. Ghodbane, PhD,[1,2] Andrzej Brzezinski, MD,[1] Jay M. Patel, PhD,[1,2] William H. Plaff, BS,[1,2] Kristen N. Marzano,[1] Charles J. Gatt, MD,[1,2] and Michael G. Dunn, PhD[1,2]

Downloaded by Univ Of Pennsylvania from www.liebertpub.com at 04/18/19. For personal use only.

Meniscal lesions represent one of the most common orthopedic injuries, and the standard of care, partial meniscectomy, often leads to long-term joint deterioration. The current meniscal replacement devices fail to recreate the native meniscus biomechanics that may explain the uncertainty of their clinical efficacy. A biomechanically functional, collagen-hyaluronan infused, three-dimensional printed polymeric scaffold was implanted into 18 sheep for up to 24 weeks to assess the scaffold's fixation, cellular response, tissue generation, integration to the host tissue, and effect on the surrounding articular cartilage. The scaffolds were assessed via gross inspection, histology, immunofluorescence, and biochemical analysis and the articular cartilage was assessed via gross inspection and histology. Scaffolds were ingrown with cells that generated a dense fibrocartilage-like tissue with significant collagen and glycosaminoglycan deposition. The stability of the surgical fixation was variable, however, with three partially displaced and five completely displaced implants at 12 weeks and three anatomic, four partially displaced, and two completely displaced implants at 24 weeks. Those implants remaining in the anatomic position displayed markedly improved outcomes. There was no significant degeneration observed in the surrounding articular cartilage for any condition. This study demonstrated the scaffold induces fibrochondrocytic tissue ingrowth, integrates robustly, and continues to mature as late as 24 weeks, and the articular cartilage is not adversely changed. The surgical model and fixation method must be improved and longer time points need to be investigated to further determine the scaffold's efficacy and chondroprotective abilities.

Keywords: knee, meniscus, tissue engineering, ovine model

Impact Statement

The only FDA-approved partial meniscus scaffold, the Collagen Meniscus Implant (CMI), is not approved for reimbursement by government and only reimbursable by certain private insurers. Scaffolds with improved mechanical properties and greater efficacy are needed. A previous study (Ghodbane, *et al.* DOI: 10.1002/jbm.b.34331) demonstrated the ability of our novel acellular, off-the shelf scaffold to restore knee biomechanics following partial meniscectomy, which could potentially decrease the risk of osteoarthritis following partial meniscectomy, providing the motivation for this study. This article presents a first-in-animal feasibility study.

Introduction

The knee meniscus is a semilunar fibrocartilaginous structure that functions in load transmission, joint stabilization, and shock absorption.[1,2] Meniscal lesions represent one of the most common orthopedic injuries[3]; however, treatment options remain inadequate due to poor healing potential in the inner, avascular body of the meniscus.[4] Partial meniscectomy provides short-term symptomatic relief but is known to increase the risk of osteoarthritis as a result of increased stresses on the articular surfaces.[5,6] Allograft transplantation represents a biomechanically functional alternative but suffers from multiple disadvantages including disease transmission, limited donor supply, size matching, and immune rejection.[7] More importantly, long-term outcomes are inconsistent due to poor tissue remodeling of the dense extracellular matrix (ECM).[8]

Therefore, researchers have investigated the possibility of meniscal regeneration either with biological (collagen,[9] hyaluronan,[10] and silk fibroin[11]) or synthetic materials (polycaprolactone [PCL],[10,12] polylactic acid,[13] poly vinyl alcohol,[14] polyglycolic acid,[15] and polyurethane[16]). Among

[1]Department of Orthopaedic Surgery, Robert Wood Johnson Medical School, Rutgers Biomedical and Health Sciences, New Brunswick, New Jersey.
[2]Department of Biomedical Engineering, Rutgers, The State University of New Jersey, Piscataway, New Jersey.

the tissue-engineered implants available in the European Union or undergoing clinical trials in the United States are the collagen meniscus implant (CMI) and Actifit, a porous polyurethane scaffold. However, the efficacy of these homogenous scaffolds remains unclear,[17] and they do not restore the natural biomechanics of the joint or prevent the development of osteoarthritis. To our knowledge, no other group has developed a meniscal scaffold that mimics the native circumferential tensile and/or axial compressive mechanics of the meniscus.

Therefore, our lab designed and optimized a device with the goal to match these properties. A three-dimensional (3D)-printed polymeric partial meniscus scaffold composed of poly(desaminotyrosyl-tyrosine dodecyl ester dodecanoate) [p(DTD DD)] infused with a collagen-hyaluronate sponge was developed and characterized to have an instantaneous compressive modulus of 109%, a time-dependent aggregate modulus of 101.5%, and a circumferential tensile modulus of 131.4% of the native ovine meniscus. In addition, the scaffold was demonstrated to improve the contact mechanics of the knee joint relative to partial meniscectomy in *in vitro* testing,[18] motivating further *in vivo* evaluation in an ovine model.

The purpose of this feasibility study was to evaluate this scaffold as a partial meniscus replacement in an ovine model. We hypothesized that a collagen-hyaluronan infused, 3D-printed polymeric partial meniscus scaffold could generate functional meniscal tissue without adversely affecting the surrounding articular surfaces. To test this hypothesis, we evaluated whether the scaffold could (1) support cell infiltration, ECM production, and organized tissue deposition, (2) integrate robustly to the surrounding native meniscal tissue, and (3) protect the articular cartilage from degeneration associated with partial meniscectomy.

Materials and Methods

Study design

Due to the anatomic similarity between ovine and human knees,[19,20] this study was performed on 24 skeletally mature male Dorset Finn Cross Sheep (2–3 years, 49–80 kg), under an approved Institutional Animal Care and Use Committee protocol (No. I13-043). Eighteen sheep received an 80% posterior meniscectomy (assuring to maintain an intact peripheral rim), representing a clinically relevant defect model,[21,22] followed by the implantation of the partial meniscus scaffold ($n=9$ at 12 and 24 weeks). Four sheep acted as 80% meniscectomy controls ($n=2$ per time point). Two sheep acted as a 24-week sham control to determine the effect of the surgical procedure alone.

The evaluation methods utilized here were adapted from those established during the development of a total meniscus scaffold.[13,23,24] At sacrifice, the synovium was assessed grossly for synovitis and articular surfaces were assessed grossly for damage and osteophyte formation. Explants were analyzed grossly for size, shape, intactness, location, and integration. Explant samples were harvested for histology, immunofluorescence, and biochemical analysis and the femoral articular surfaces were evaluated histologically.

Scaffold fabrication

Eighteen meniscus scaffolds were fabricated as previously described.[18] p(DTD DD) was 3D printed at 160°C and 1.2 mm/s on a 3D Bioplotter (EnvisionTEC, Dearborn, MI) at the New Jersey Center for Biomaterials (Department of Chemistry, Rutgers University, Piscataway, NJ). Sodium hyaluronate (0.25 g/L; molecular weight 1.5–2.2 MDa) was dissolved in dilute hydrochloric acid (pH 2.35). Lyophilized bovine Achilles tendon collagen (Worthington Biochemical Corporation, Lakewood, NJ) was swollen in the hyaluronate solution at 20 g/L. The dispersion was infused into the void space of the polymeric structure, frozen via ethanol-dry ice bath for 30 min, and lyophilized. Scaffolds were cross-linked with 10 mM, 1-ethyl-3-(3-dimethaylaminopropyl)carbodiimide hydrochloride and 5 mM, N-hydroxysuccinimide for 6 h, subjected to 3, 10-min DI H_2O rinses, a 3-h 100 mM sodium phosphate rinse, and 4, 6 h DI H_2O rinses. Scaffolds were subsequently frozen, lyophilized, and sterilized with 25 kGy of gamma irradiation (Sterigenics, Rockaway, NJ).

Surgical procedure and sacrifice

Animals were induced with a ketamine-xylazine-midazolam cocktail, intubated, and the right hind leg was prepared for surgery. A modified medial parapatellar arthrotomy and epicondylar osteotomy were performed to provide access to the medial compartment. The medial meniscus was exposed, and an 80% posterior meniscectomy was performed with care taken to maintain the integrity of the peripheral rim (Fig. 1). Using the excised tissue as a template, the scaffold was trimmed to the correct shape, hydrated in saline, and reduced. The scaffold was sutured with two radial 2-0 Ethibond (Ethicon, Somerville, NJ) vertical mattress sutures tied over the joint capsule and two circumferential 3-0 PDS (Ethicon) simple sutures. The meniscus was restored to the proper position and the osteotomy was fixed using a 3.5 mm cortical screw (Synthes, Monument, CO). The capsule, fascia, and skin were closed. Animals were recovered in cages without limitations on movement. Animals were sent to a farm facility $\sim$10 days postoperatively, and were sacrificed at 12 or 24 weeks.

Scaffold histological analysis

Immediately after dissection, the medial meniscus was severed at the roots, the scaffold was located, and a slice was taken through the width of the scaffold and native outer rim. The section was fixed in 10% Carson buffered formalin, embedded in paraffin, and cut into 8-mm cross sections. The sections were stained with hematoxylin and eosin (H&E), Safranin-O/Fast Green, or Picrosirius Red (AML Laboratory, Saint Augustine, FL). Sections were assessed for the magnitude and type of tissue ingrowth, tissue thickness and integrity, surface features, cell density, vascularization, and inflammatory response.

Immunofluorescence

One mm-thick cross-sectional slices were excised from the scaffold and the posterior region of the contralateral meniscus. The sections were embedded in Optimal Cutting Temperature compound (Tissue-Tek; Sakura, Torrance, CA), chilled on ice, flash frozen in liquid nitrogen, and

Downloaded by Univ Of Pennsylvania from www.liebertpub.com at 04/18/19. For personal use only.

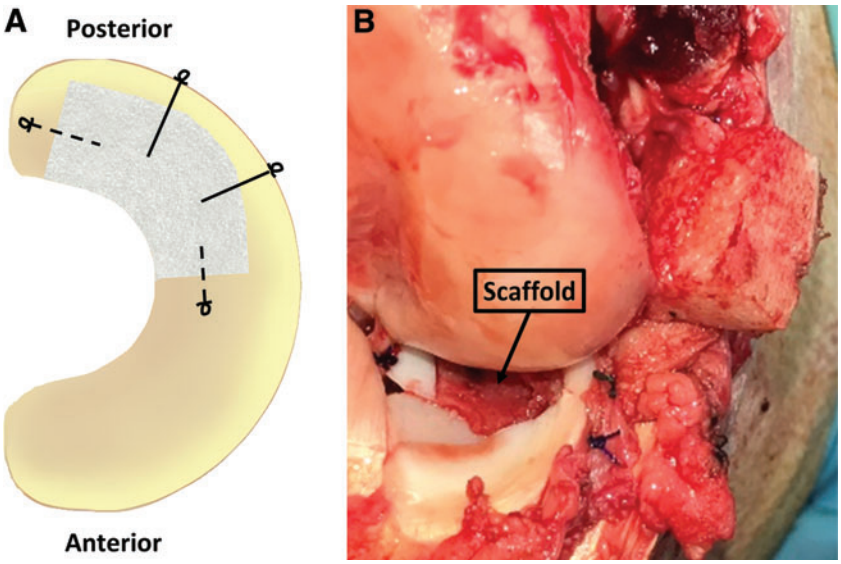

FIG. 1. **(A)** Scaffold fixation scheme. *Solid lines* represent 2-0 Ethibond sutures and *dashed lines* represent 3-0 PDS sutures. Suture knot locations are depicted by loops. **(B)** Implanted scaffold after meniscus was restored to the proper position. Color images are available online.

Downloaded by Univ Of Pennsylvania from www.liebertpub.com at 04/18/19. For personal use only.

stored at −80°C. Ten μm slices were cut using a cryostat, placed on microscope slides, and dried at room temperature. Rabbit Type I Collagen antibody (AB745; Millipore, Billerica, MA) with a 1:300 dilution and Rabbit Type II Collagen antibody (AB34712; Abcam, Inc., Cambridge, MA) with a dilution of 1:200 were applied to the tissue. The secondary Antibody was Donkey-anti-rabbit AlexaFluor 594 Texas Red (Invitrogen) with a dilution of 1:1000. Samples were mounted with Anti-Fade ProLong Gold with DAPI for nucleus visualization and imaged with a Leica fluorescent microscope with a ProgRes camera and CapturePro imaging software (Jenoptik Laser, Jena, Germany).

Biochemical composition analysis

Collagen and sulfated-glycosaminoglycans (S-GAGs) were quantified via biochemical assays. One millimeter cross sections were taken from the scaffold or inner margin of native tissues at sacrifice and were fresh frozen. On the day of testing, the samples were thawed and hydrated in phosphate-buffed saline (PBS). The samples were superficially dried, weighed (hydrated mass), lyophilized, and weighed (dry weight). Samples were digested in papain solution (1 mg tissue/100 μL solution; 125 mg/mL papain, 5 mM L-cysteine-HCl, 5 mM ethylenediaminetetraacetic acid disodium in PBS [pH = 7.4]) for 24 h at 37°C. A portion of the sample homogenate was set aside and a portion was diluted 1:2 in 12 M HCl at 120°C for 24 h to hydrolyze the sample. The hydrolyzed samples were diluted 1:3 in 6 M HCl and the homogenates were diluted 1:4 to bring the concentrations to an appropriate range for each assay.

Water content was defined as the ratio of the hydrated weight to dry weight. Collagen content was assessed using a hydroxyproline assay kit (Cat. No. 6017; Chondrex, Inc.) on the hydrolyzed samples and S-GAG content was assessed using a glycosaminoglycan assay kit (Cat. No. 6022; Chondrex, Inc.) on the sample homogenates, according to the manufacturer's instructions. For collagen content, hydroxyproline content was converted to collagen content using a scale factor of 7.46.[25]

Cartilage histological analysis

Femoral condyles were evaluated histologically. Three mediolateral slices were taken from the anterior, central, and posterior regions of the surgical and contralateral joints. The slices were fixed in 10% Carson's buffered formalin, decalcified with acid-EDTA solution, paraffin-embedded, sectioned to 8 μm, and stained with Safranin O/Fast Green (AML Laboratories). Each section was further divided into three regions (medial, central, and lateral) to obtain nine regions per medial femoral condyle according to the ICRS mapping scheme.[26] Sections were graded using a single-blind modified microscopic scoring system from OARSI[27] by three independent observers. The OARSI system includes weighted scoring for structure, chondrocyte density, cell cloning, Safranin-O retention, and tidemark integrity with a maximum score of 25.

Statistical analysis

Statistical analyses were performed with Minitab software (v 18.1; Minitab, Inc.). A two-way analysis of variance with a *post hoc* Tukey method was performed to compare the biochemical data. Although these data were not normal, the OARSI histological scoring data did possess equal variance; therefore, a three-way analysis of variance with a *post hoc* Tukey method was used after removing outliers. A p-value of <0.05 was considered significant.

Results

Macroscopic observations

All animals returned to an unrestricted, standing position within 4 h postoperatively and achieved normal weight bearing by 8 weeks. The animals experienced an average of 5.6% weight gain by the conclusion of the study. One animal from the 12-week experimental group expired 4 days postoperation due to gastrointestinal complications.

At sacrifice, some discoloration and thickening of the synovium was observed in both experimental and sham joints. At 12-week sacrifice, three scaffolds were completely

displaced from the joint into the knee capsule and five had partially displaced from the implantation site but remained within the joint. The completely displaced scaffolds appeared to have overturned, rotating about the outer meniscal rim. The partially displaced scaffolds were extruded underneath the native meniscus and, to varying extents, migrated posteriorly. At 24-week sacrifice, three scaffolds had successfully retained anatomic placement, four were partially displaced, and two completely displaced (Fig. 2). We used the three outcomes of the surgery as an opportunity to understand the effect of the biomechanical environment on tissue formation within the scaffolds. Therefore, from this point forward, we analyzed the scaffolds according to the three subgroups: anatomic, partially displaced, and completely displaced.

All anatomic and partially displaced scaffolds experienced significant tissue infiltration, exhibited the texture of a meniscus reinforced with stiff polymer when compressed, and appeared whiter in color than the native meniscus. There was robust tissue integration with the remaining host tissue in the red-red and red-white zones. No decrease in scaffold volume from time of implantation to sacrifice was observed. At 12 weeks, two partially displaced scaffolds and one completely displaced scaffold had fragmented into two parts. This was not observed at 24 weeks. The completely displaced scaffolds exhibited more signs of wear, some tissue ingrowth, and integrated strongly to the capsule. In the meniscectomy controls, the remaining meniscal tissue deformed into a triangular shape with a thin, translucent tip toward the inner margin. However, this did not correspond to an increase in meniscal volume.

Articular surfaces from the contralateral knee exhibited mild surface roughening without any osteophytes (Fig. 3). The joints from the sham subjects had similar surface roughening and mild osteophyte development. All surgical knees demonstrated slightly increased surface roughening, relative to the sham, with some fibrillation and fissures observed. There was no macroscopic difference in cartilage health between the 12 and 24-week time points. Osteophyte formation was similar between all surgical joints, including the 24-week sham, 12-week scaffolds, and the anatomic 24-week scaffolds. Moderate osteophyte development was observed in knees corresponding to the 24-week partially and completely displaced scaffolds.

Scaffold histology

Histological evaluation revealed all scaffolds maintained their original thickness, did not adversely affect adjacent tissue, and experienced tissue ingrowth throughout without any large pores or gaps. Anatomic and partially displaced scaffolds exhibited dense tissue infiltration and growth at both 12 and 24 weeks with hypercellularity relative to native tissue (Fig. 4A). In anatomic scaffolds, no obvious interface between the scaffold and the host tissue could be discerned due to the extent of tissue ingrowth (Fig. 2). A mixed population of elongated and round cells were observed with a larger proportion of round cells at 24 weeks. The cells exhibited a normal cell morphology with some instances of cell clustering that were associated with a deeper Safranin-O staining (Fig. 4B). Vascularization was found throughout scaffolds at 12 and 24 weeks, and only in the outer margin of native menisci. Focal clusters of lymphocytes and relatively few multinucleated giant cells were observed at both time points (Fig. 4A). The tissue developed large collagenous bundles running radially with larger bundles at 24 weeks, as shown by intense PicroSirus Red staining (Fig. 4B). Some Safranin-O staining was observed in all scaffolds within the joint with a slight increase observed between 12 and 24 weeks.

Immunofluorescence

Immunofluorescence staining showed COL-I was throughout the scaffolds with a greater intensity on the surface and surrounding large fibers (dark voids). Cell nuclei found near COL-I staining were typically more elongated than cells found near COL-II staining (Fig. 5). COL-I was observed to a much greater extent in completely displaced scaffolds. Anatomic scaffolds exhibited the least staining,

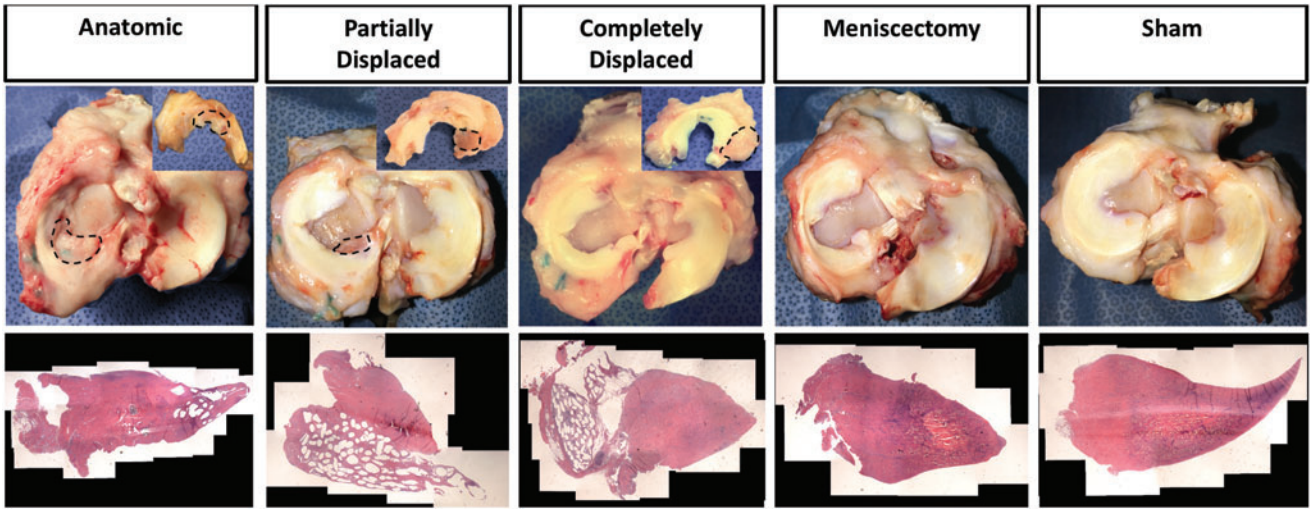

FIG. 2. Representative gross appearance from top and bottom view (*inset*) of meniscus. Scaffolds are *circled* with *black dotted line*. H&E composite image (20×) from each outcome are below gross images. H&E, hematoxylin and eosin. Color images are available online.

Downloaded by Univ Of Pennsylvania from www.liebertpub.com at 04/18/19. For personal use only.

Downloaded by Univ Of Pennsylvania from www.liebertpub.com at 04/18/19. For personal use only.

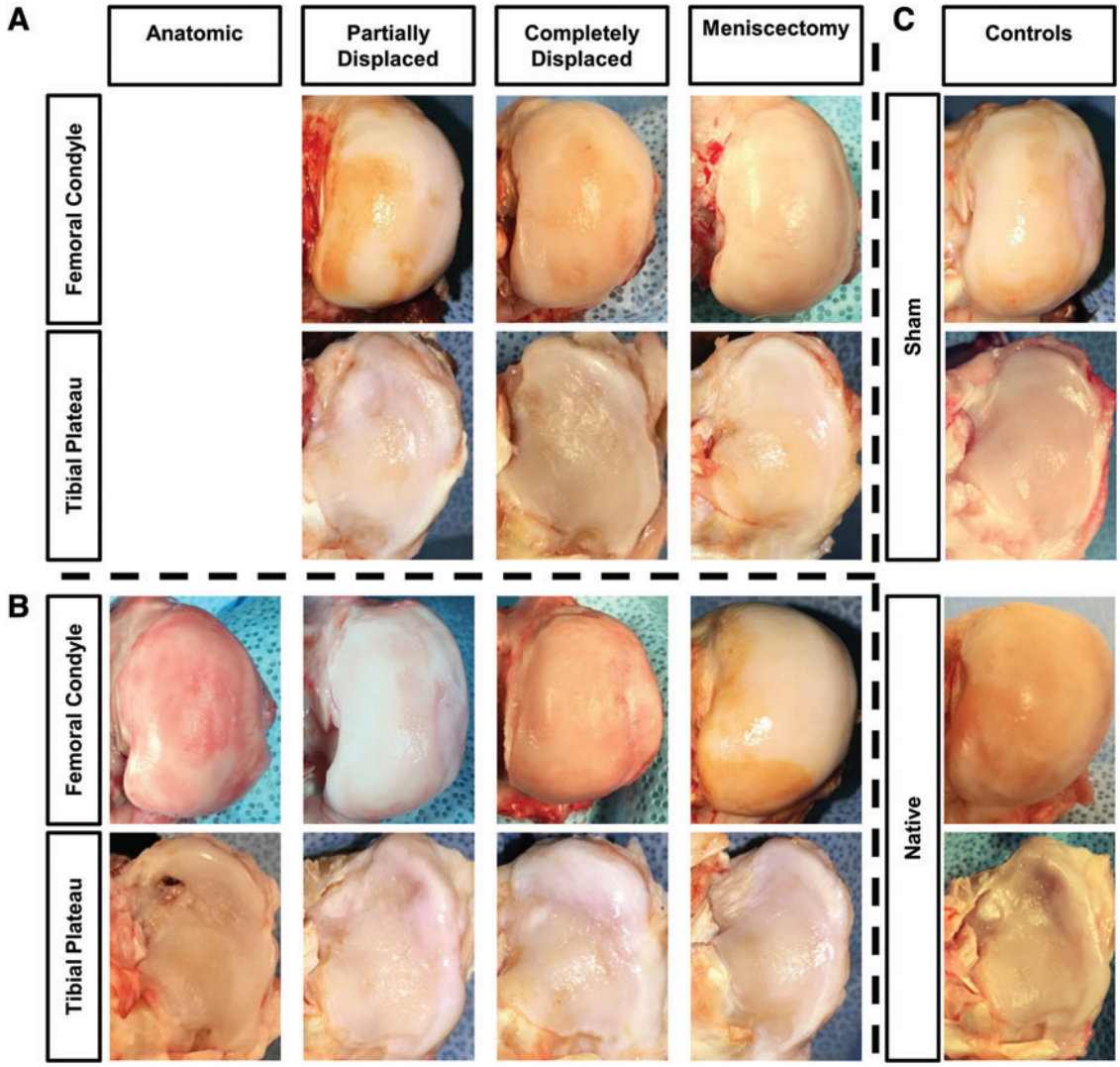

FIG. 3. Representative gross appearance of femoral condyle and tibial plateau articular surfaces from each outcome at **(A)** 12 weeks and **(B)** 24 weeks, and **(C)** for sham and native controls. Color images are available online.

relative to other scaffolds, but more than native controls. In partially displaced and anatomic scaffolds, COL-I organization typically ran concentrically around the polymer fibers and intensity decreased from 12 to 24 weeks. Native samples only exhibited minor COL-I staining at the tissue surface.

COL-II was found throughout all anatomic and partially displaced scaffolds with round cell nuclei adjacent to the intense staining. At 24 weeks, anatomic scaffolds exhibited higher staining intensity relative to partially displaced scaffolds at equivalent time points. A small increase in intensity was observed from 12 to 24 weeks for all scaffold groups. Negligible staining was detected in completely displaced scaffolds.

Biochemical composition

There were no significant differences in water content between each condition ($p=0.59$) or time points ($p=0.72$) (Fig. 6A). Native menisci had significantly greater collagen and GAG content than all scaffold groups (Fig. 6B, C). The outcome of the scaffold had a direct effect on the collagen and GAG content of the scaffold. Anatomic scaffolds possessed nearly identical collagen content at 24 weeks as partially displaced scaffolds, corresponding to more than a third of the value for contralateral controls. On the other hand, the anatomic scaffolds developed nearly 40% more GAGs than the partially displaced scaffolds at 24 weeks. Partially displaced scaffolds developed $15.5\% \pm 7.7\%$ collagen content at 12 weeks and continued to increase to $22\% \pm 0.7\%$ at 24 weeks. The partially displaced and anatomic scaffolds achieved 53% and 74% of the GAG concentration of contralateral menisci, respectively. For completely displaced scaffolds, collagen content was $12.8\% \pm 4.9\%$ at 12 weeks and did not increase further at 24 weeks ($11.4\% \pm 0.1\%$). GAG content demonstrated a similar trend with a content <40% of the contralateral control at 12 weeks with no increase from 12 to 24 weeks.

Cartilage histology

The contralateral femoral surfaces experienced minor surface disruptions, normal Safranin-O staining, normal cell density and cloning, and an uninterrupted tidemark (Fig. 7).

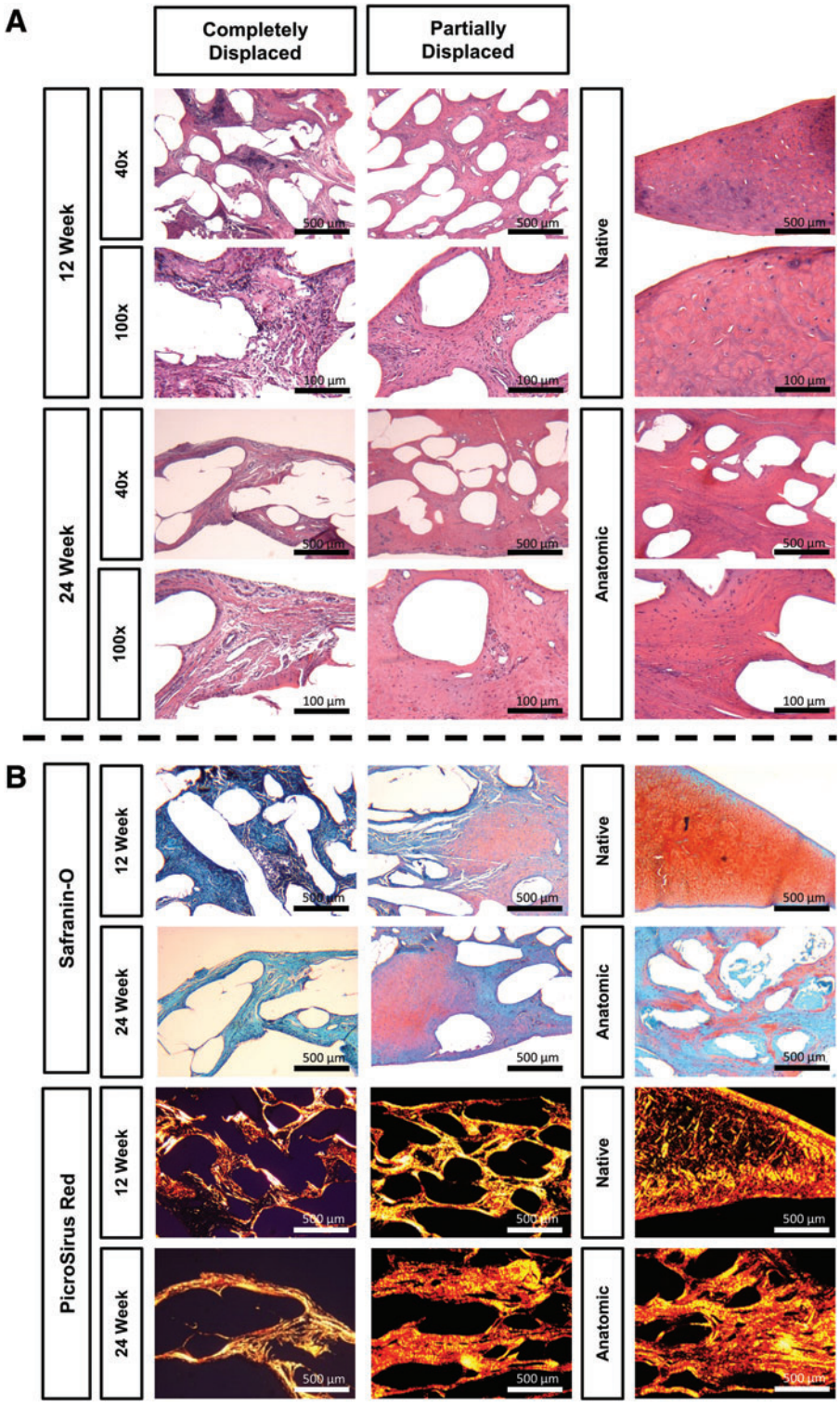

FIG. 4. **(A)** H&E images of scaffolds and contralateral controls. Image magnification: 40× and 100×. Scale bars: 500 and 100 µm. **(B)** Safranin-O/Fast Green and Picrosirus Red images of scaffolds and contralateral controls. Image magnification: 40×. Scale bars: 500 µm. Color images are available online.

The sham surfaces exhibited moderate surface irregularities and very mild cell cloning. The 12 and 24 week meniscectomy surfaces had severe surface irregularities, a slight decrease in cell density, moderate cell cloning, and normal Safranin-O staining.

The cartilage damage was least for the joints corresponding to anatomic scaffolds, followed by partially displaced, and completely displaced experienced the most damage. Articular surfaces from anatomic scaffolds typically exhibited mild surface disruption, normal cell density, Safranin-O staining, mild cell cloning, and an uninterrupted tidemark (Fig. 7). Joints with partially displaced scaffolds were slightly hypocellular and had mild cell cloning at both time points but advanced from moderate to severe surface irregularities with some fissures to the transitional zone from 12 to 24 weeks. The cartilage from joints with completely

Downloaded by Univ Of Pennsylvania from www.liebertpub.com at 04/18/19. For personal use only.

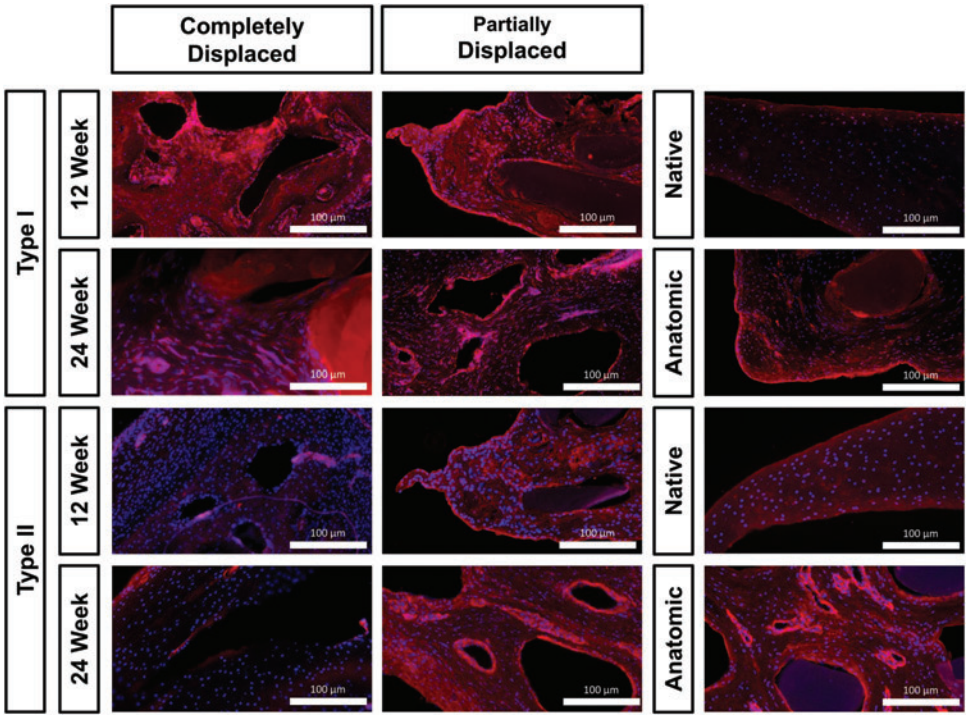

FIG. 5. Type I and II collagen immunofluorescence at 100×. *Red* indicates collagen presence and *blue* indicates cell nuclei. Scale bar: 100 µm. Color images are available online.

displaced scaffolds experienced severe surface irregularities at 12 weeks and fissures down to the transitional zone at 24 weeks, in addition to a hypocellularity and mild cell cloning.

OARSI cartilage damage scores (Fig. 7) did not show large differences between groups. The score did not significantly increase ($p = 0.093$) from 12 to 24 weeks and there was not a significant difference in average damage between the anatomic scaffolds, partial meniscectomy, sham, and contralateral conditions with averages ranging from 6.2 to 7.7. The partially and completely displaced scaffolds resulted in significantly increased cartilage damage relative to the contralateral controls with averages of 8.3 and 8.8, respectively.

Discussion

The purpose of this pilot study was to assess the feasibility of using a novel 3D printed, mechanically functional, polymeric scaffold in a short-term partial meniscus replacement model. We unexpectedly observed three different outcomes for the scaffold; however, this provided a unique insight into the performance of this device. We observed differences in the three outcomes with regards to tissue ingrowth, type, organization, density, and biochemical composition. The anatomic scaffolds induced significant tissue ingrowth, remodeled into neo-meniscal tissue, integrated robustly to the host meniscal tissue, and did not adversely affect the articular cartilage of the joint.

Significant tissue ingrowth was found within all scaffolds. The original porous collagen matrix was completely remodeled into a dense ECM with cells exhibiting both a fibroblastic and fibrochondrocytic morphology. Interestingly, the type of tissue ingrowth was directly dependent on the location of the scaffold. Those scaffolds that had remained in place (anatomic) were presumably exposed to the appropriate biochemical and mechanical stimuli, resulting in fibrocartilage-like tissue; in contrast, partially displaced scaffolds exhibited a range of fibrous to fibrocartilage-like tissue, and completely displaced scaffolds had developed loose, fibrous connective tissue.

The quality of tissue observed in the scaffolds was typically denser and more organized than tissue generated from previously reported scaffolds lacking biological enhancement at equivalent time points.[11,12,16,28] CMI exhibited bands of unorganized connective tissue with fibroblasts, capillaries, and fine collagen fibers in mixed breed dogs at 12 weeks. At 24 weeks, the collagen fibers had grown in diameter and became more organized but islands of the cross-linked collagen scaffold material remained.[28] At 12 weeks, Actifit remained relatively porous and lacked any clear organization.[16] Gruchenberg *et al.* observed pores up to 10 µm in diameter that were empty or filled with amorphous material in a silk fibroin scaffold at 12 and 24 weeks.[11] A 3D-printed PCL scaffold, when growth factors were not added, only developed an amorphous fibrous tissue at 12 weeks resembling the tissue quality of the completely displaced scaffolds in this study.[12] The relatively dense and organized tissue observed in this study without the addition of any biological factors is most like the result of the similarity of the mechanical properties of the scaffold relative to the native meniscal tissue.

The ability of a scaffold to integrate to the remaining meniscal tissue is essential for the success of a partial meniscus scaffold and may be enhanced with ECM-derived materials. The integration observed in this study in anatomical and partially displaced scaffolds was quite robust as early as 12 weeks with little distinguishable interface between the neo- and host tissue. Although, this integration occurred on unexpected surfaces in partially displaced scaffolds (i.e., the upper surface of the scaffold to the lower surface of the meniscus). In CMI, integration does not occur

Downloaded by Univ Of Pennsylvania from www.liebertpub.com at 04/18/19. For personal use only.

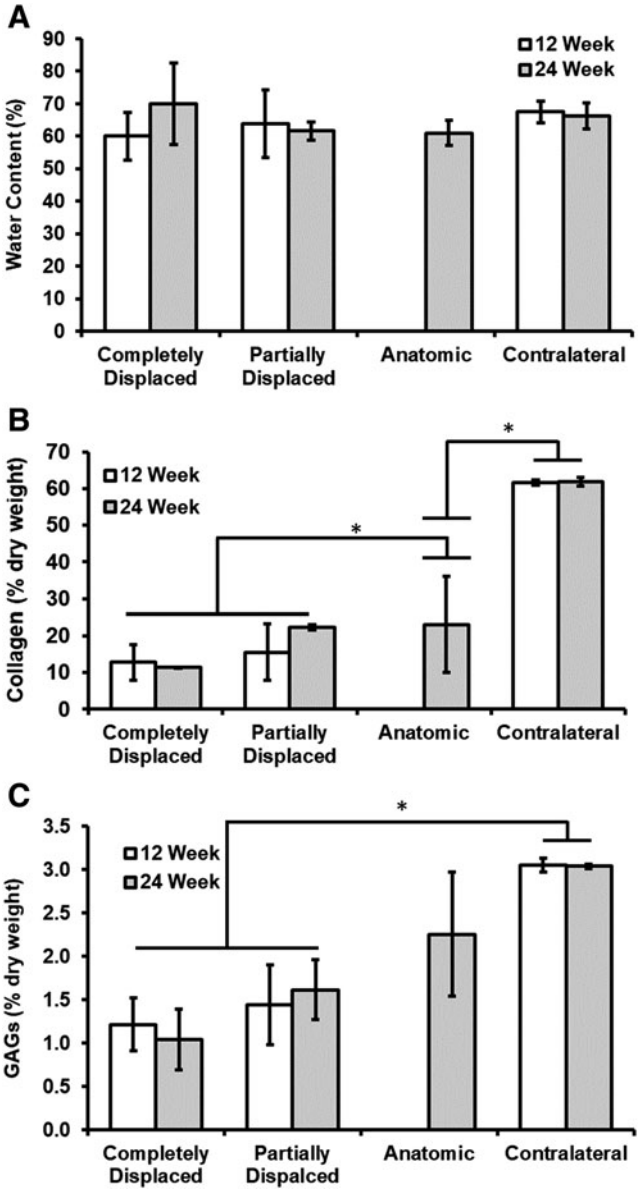

FIG. 6. Biochemical composition of scaffolds and contralateral controls. **(A)** Water content, **(B)** collagen content, and **(C)** sulfated-GAGs. Collagen and sulfated-GAGs expressed as a percentage of dry weight tissue. Values indicated are mean ± SD. *Asterisk* denotes statistically significant differences ($p < 0.05$). GAGs, glycosaminoglycans; SD, standard deviation.

up to 6 weeks but is robust by 52 weeks.[29] PCL-hyaluronan scaffolds resulted in some fibrous ingrowth in two out of three cases in a partial, segmental defect but the interface was noticeably less dense than the rest of the generated tissue.[30] Actifit, a synthetic scaffold, integrates less reliably with only four out of seven scaffolds well-integrated as late as 52 weeks in one study[16] and silk fibroin scaffolds left a large gap between the scaffold and host tissue with no signs of fibrous adhesion as late as 24 weeks.[11]

The scaffold demonstrated a lymphocytic response, similar to other collagenous scaffolds.[28,31] Relatively few multinucleated giant cells were observed relative to other synthetic meniscal scaffolds developed in the past,[32–34] suggesting the scaffold material was well tolerated. Clusters of cartilaginous differentiation have been observed in PCL-hyaluronan scaffolds, but only when seeded with cells.[33] Our scaffolds developed fibrocartilaginous tissue without cell seeding or growth factors, suggesting the mechanical environment influenced the cellular response, consistent with previous *in vitro*[35] and *in vivo*[36] studies. Vascularization was observed throughout the scaffold similar to our laboratory's total meniscus replacement device at similar time points.[23]

The biochemical composition of the native meniscus dictates its biomechanical function. The collagen provides the tensile properties and the GAGs increase the ability of the tissue to absorb and retain water, improving the viscoelastic compressive properties.[37] The outcome of each scaffold had a direct effect on the biochemical development of the scaffold with the anatomic scaffolds achieving the best biochemical composition. The biochemical data in this study further confirmed that the anatomic scaffolds are maturing toward a fibrocartilaginous tissue up to 24 weeks. The contralateral controls were consistent with previous values from the literature of 68% water content[19] and 60–70% collagen[38]; however, the GAG content in this study (3%) was greater than previous values of 1–2% GAGs,[4,24] perhaps because samples were taken exclusively from the inner margin and previously reported values were an average of the whole tissue.[39]

We characterized the gross and histological changes of the articular surfaces to determine effects of the surgery and the scaffold on the surrounding cartilage. Compared to contralateral controls, a significant increase in the OARSI score was found in knees with partially and completely displaced scaffolds. There was no significant change between the contralateral, sham, meniscectomy, and anatomic scaffolds and no change from 12 to 24 weeks. This is likely the result of the partial, posterior defect model at short time points. Although past studies performed in our laboratory utilizing a total meniscectomy defect model observed significant gross articular degradation as early as 16 weeks,[23] a less significant damage would be expected from a partial defect model considering it is well established clinically that partial meniscectomies result in better outcomes than total menisectomies.[6] This is consistent with findings in the literature that used similar defect models.[11,16] Gruchenberg *et al.* found, when excluding outliers, there was little change in the macroscopic area of cartilage damage and the mechanics of the cartilage did not change in the region underneath a silk fibroin scaffold.[11] However, they did observe some degenerative changes via histology including some fibrillation, a reduction in Safranin-O staining, and cell cloning in the experimental joints. Maher *et al.* also did not observe adverse changes in cartilage histological scoring between 12 and 24 weeks.[16]

The geometry of our defect and surgical fixation proved to be shortcomings of this pilot study, with the majority of the scaffolds displaced. In an effort for a highly reproducible defect model, we chose a model with right angles and predefined dimensions; however, this may have resulted in the remaining native meniscal tissue deforming due to stress concentrations. We recommend changing the size and shape of the meniscal defect in future studies to avoid these problems.

Downloaded by Univ Of Pennsylvania from www.liebertpub.com at 04/18/19. For personal use only.

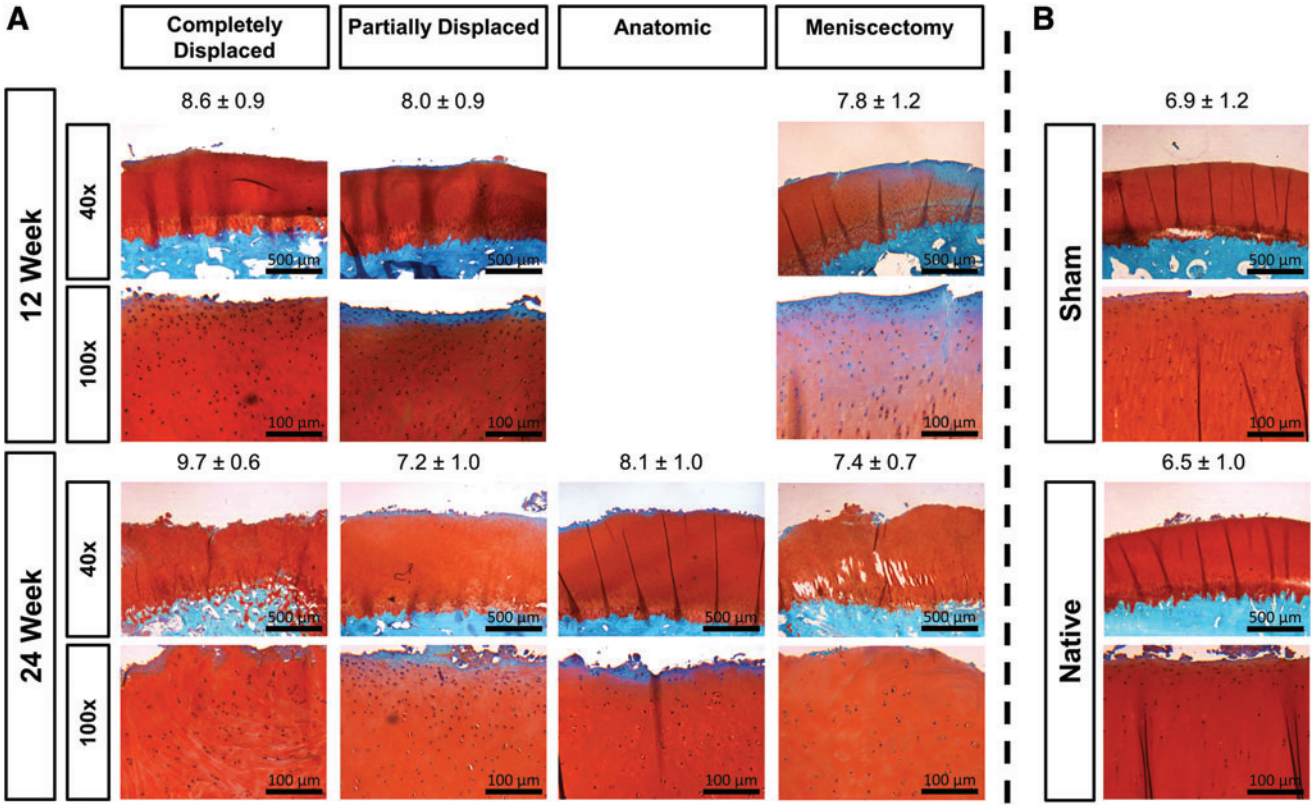

FIG. 7. Representative cartilage histology and OARSI scores. Femoral condyle cartilage stained with Safranin-O/Fast Green from knees with **(A)** scaffolds and **(B)** controls. Image magnification: 40× and 100×. Scale bars: 500 and 100 µm. OARSI cartilage damage scores are represented by mean ± SD. Color images are available online.

The animal model simulates a worst-case scenario with regards to the rehabilitation protocol. The animals were standing 4 h postoperatively, potentially leading to early displacement of the scaffold. In humans, a strict toe-touch weight bearing protocol would be in place for 4 weeks before returning to weight bearing. This allows for early tissue infiltration and integration to occur before subjecting the scaffold to significant loads. Considering our small number in each group and the observation that all anatomic scaffolds were harvested at the longer time point suggests there is a critical early time frame during which the scaffold must remain in place for long-term success.

We hypothesize the fixation failure begins with the failure of the anterior circumferential suture from the shear force as a result flexion/extension, causing a tendency to separate the scaffold from the anterior portion of the meniscus. This allows the scaffold to move more freely in the joint resulting in either the extrusion of the scaffold underneath the host tissue (as in the case of the partially displaced scaffolds) or rotation of the entire scaffold over the meniscal rim and into the knee capsule (completely displaced scaffolds). The circumferential sutures were PDS to minimize the cartilage damage caused by the presence of a knot within the joint. The fixation can be improved by placing exclusively radial sutures that are not susceptible to the same phenomenon and can be knotted outside of the joint capsule.

This was a first in-animal, feasibility study that suffered from a few limitations. First, this study was performed with a relatively small sample size in efforts to reduce the use of animals. Additionally, the time points were too short to assess the chondroprotective abilities of our scaffold. Finally, no biomechanical testing was performed as the amount of tissue available per animal was extremely limited.

This study demonstrated a collagen-hyaluronan infused 3D-printed polymeric scaffold could induce significant fibrochondrocytic tissue ingrowth, integrate robustly, and continue to mature as late as 24 weeks without adversely affecting the articular cartilage of the joint. However, surgical fixation of the scaffold to the remaining native meniscal rim was inconsistent. Future work will explore a modified fixation method for longer time points to assess the continued remodeling of the tissue and the scaffold's ability to protect the underlying articular cartilage.

Acknowledgments

The authors thank the staff of the Department of Orthopaedic Surgery, specifically Barbara Perry, and Comparative Medicine Resources at Rutgers Biomedical and Health Sciences for their help with the animal surgery, postoperative care, and sacrifice. The authors thank Dr. Joachim Kohn and New Jersey Center for Biomaterials for synthesizing polymer and providing the facilities for 3D printing, Drs. Marion Gordon and Rita Hahn for their assistance with immunofluorescence. The research herein was funded by the Armed Forces Institute for Regenerative Medicine II (AFIRM II; grant W81XWH-08-2-0034).

Downloaded by Univ Of Pennsylvania from www.liebertpub.com at 04/18/19. For personal use only.

Downloaded by Univ Of Pennsylvania from www.liebertpub.com at 04/18/19. For personal use only.

Disclosure Statement

The meniscus device described in this article has one patent pending (PCT/US18/17988). The technology has been licensed for product development (MeniscoFix, NovoPedics, Inc.). J.M.P. serves as a consultant for NovoPedics, Inc. C.J.G. serves as interim president and owns stock in NovoPedics, Inc. M.G.D. serves as interim secretary and treasurer and owns stock in NovoPedics, Inc.

References

1. Makris, E.A., Hadidi, P., and Athanasiou, K.A. The knee meniscus: structure-function, pathophysiology, current repair techniques, and prospects for regeneration. Biomaterials **32**, 7411, 2011.
2. Fithian, D.C., Kelly, M.A., and Mow, V.C. Material properties and structure-function relationships in the menisci. Clin Orthop Relat Res **19,** 1990.
3. Garrett, W.E., Jr., Swiontkowski, M.F., Weinstein, J.N., *et al.* American Board of Orthopaedic Surgery Practice of the Orthopaedic Surgeon: part-II, certification examination case mix. J Bone Joint Surg Am **88**, 660, 2006.
4. Fox, A.J., Bedi, A., and Rodeo, S.A. The basic science of human knee menisci: structure, composition, and function. Sports Health **4**, 340, 2012.
5. Northmore-Ball, M.D., Dandy, D.J., and Jackson, R.W. Arthroscopic, open partial, and total meniscectomy. A comparative study. J Bone Joint Surg Br **65**, 400, 1983.
6. Papalia, R., Del Buono, A., Osti, L., Denaro, V., and Maffulli, N. Meniscectomy as a risk factor for knee osteoarthritis: a systematic review. Br Med Bull **99**, 89, 2011.
7. Vangsness, C.T., Jr., Garcia, I.A., Mills, C.R., Kainer, M.A., Roberts, M.R., and Moore, T.M. Allograft transplantation in the knee: tissue regulation, procurement, processing, and sterilization. Am J Sports Med **31**, 474, 2003.
8. Noyes, F.R., and Barber-Westin, S.D. Long-term survivorship and function of meniscus transplantation. Am J Sports Med **44**, 2330, 2016.
9. Martinek, V., Ueblacker, P., Bräun, K., *et al.* Second generation of meniscus transplantation: in-vivo study with tissue engineered meniscus replacement. Arch Orthop Trauma Surg **126**, 228, 2006.
10. Kon, E., Filardo, G., Tschon, M., *et al.* Tissue engineering for total meniscal substitution: animal study in sheep model—results at 12 months. Tissue Eng Part A **18**, 1573, 2012.
11. Gruchenberg, K., Ignatius, A., Friemert, B., *et al.* In vivo performance of a novel silk fibroin scaffold for partial meniscal replacement in a sheep model. Knee Surg Sports Traumatol Arthrosc **23**, 2218, 2015.
12. Lee, C.H., Rodeo, S.A., Fortier, L.A., Lu, C., Erisken, C., and Mao, J.J. Protein-releasing polymeric scaffolds induce fibrochondrocytic differentiation of endogenous cells for knee meniscus regeneration in sheep. Sci Transl Med **6**, 266ra171, 2014.
13. Patel, J.M., Merriam, A.R., Kohn, J., Gatt, C.J., Jr., and Dunn, M.G. Negative outcomes of poly(L-lactic acid) fiber-reinforced scaffolds in an ovine total meniscus replacement model. Tissue Eng Part A **22**, 1116, 2016.
14. Kobayashi, M., Chang, Y.S., and Oka, M. A two year in vivo study of polyvinyl alcohol-hydrogel (PVA-H) artificial meniscus. Biomaterials **26**, 3243, 2005.
15. Kang, S.W., Son, S.M., Lee, J.S., *et al.* Regeneration of whole meniscus using meniscal cells and polymer scaffolds in a rabbit total meniscectomy model. J Biomed Mater Res A **77a**, 659, 2006.
16. Maher, S.A., Rodeo, S.A., Doty, S.B., *et al.* Evaluation of a porous polyurethane scaffold in a partial meniscal defect ovine model. Arthroscopy **26**, 1510, 2010.
17. Houck, D.A., Kraeutler, M.J., Belk, J.W., McCarty, E.C., and Bravman, J.T. Similar clinical outcomes following collagen or polyurethane meniscal scaffold implantation: a systematic review. Knee Surg Sports Traumatol Arthrosc 26, 2259, 2018.
18. Ghodbane, S.A., Patel, J.M., Brzezinski, A., Lu, T.M., Gatt, C.J., and Dunn, M.G. Biomechanical characterization of a novel collagen-hyaluronan infused 3D-printed polymeric device for partial meniscus replacement. J Biomed Mater Res B [In Press].
19. Brzezinski, A., Ghodbane, S.A., Patel, J.M., Perry, B.A., Gatt, C.J., and Dunn, M.G. The ovine model for meniscus tissue engineering: considerations of anatomy, function, implantation, and evaluation. Tissue Eng Part C Methods **23**, 829, 2017.
20. Chevrier, A., Nelea, M., Hurtig, M.B., Hoemann, C.D., and Buschmann, M.D. Meniscus structure in human, sheep, and rabbit for animal models of meniscus repair. J Orthop Res **27**, 1197, 2009.
21. Roos, H., Laurén, M., Adalberth, T., Roos, E.M., Jonsson, K., and Lohmander, L.S. Knee osteoarthritis after meniscectomy: prevalence of radiographic changes after twenty-one years, compared with matched controls. Arthritis Rheum **41**, 687, 1998.
22. Smith, J.P., 3rd, and Barrett, G.R. Medial and lateral meniscal tear patterns in anterior cruciate ligament-deficient knees. A prospective analysis of 575 tears. Am J Sports Med **29**, 415, 2001.
23. Merriam, A.R., Patel, J.M., Culp, B.M., Gatt, C.J., and Dunn, M.G. Successful total meniscus reconstruction using a novel fiber-reinforced scaffold. Am J Sport Med **43**, 2528, 2015.
24. Patel, J.M., Merriam, A.R., Culp, B.M., Gatt, C.J., and Dunn, M.G. One-year outcomes of total meniscus reconstruction using a novel fiber-reinforced scaffold in an ovine model. Am J Sports Med **44**, 898, 2016.
25. Neuman, R.E., and Logan, M.A. The determination of hydroxyproline. J Biol Chem **184**, 299, 1950.
26. Brittberg, M., and Winalski, C.S. Evaluation of cartilage injuries and repair. J Bone Joint Surg Am **85-A**(Suppl 2), 58, 2003.
27. Little, C.B., Smith, M.M., Cake, M.A., Read, R.A., Murphy, M.J., and Barry, F.P. The OARSI histopathology initiative—recommendations for histological assessments of osteoarthritis in sheep and goats. Osteoarthritis Cartilage **18**(Suppl 3), S80, 2010.
28. Stone, K.R., Rodkey, W.G., Webber, R., McKinney, L., and Steadman, J.R. Meniscal regeneration with copolymeric collagen scaffolds. In vitro and in vivo studies evaluated clinically, histologically, and biochemically. Am J Sports Med **20**, 104, 1992.
29. Hansen, R., Bryk, E., and Vigorita, V. Collagen scaffold meniscus implant integration in a canine model: a histological analysis. J Orthop Res **31**, 1914, 2013.
30. Chiari, C., Koller, U., Dorotka, R., *et al.* A tissue engineering approach to meniscus regeneration in a sheep model. Osteoarthritis Cartilage **14**, 1056, 2006.
31. Cook, J.L., Tomlinson, J.L., Arnoczky, S.P., Fox, D.B., Reeves Cook, C., and Kreeger, J.M. Kinetic study of the replacement of porcine small intestinal submucosa grafts

and the regeneration of meniscal-like tissue in large avascular meniscal defects in dogs. Tissue Eng **7**, 321, 2001.
32. Tienen, T.G., Heijkants, R.G., de Groot, J.H., *et al.* Replacement of the knee meniscus by a porous polymer implant: a study in dogs. Am J Sports Med **34**, 64, 2006.
33. Kon, E., Chiari, C., Marcacci, M., *et al.* Tissue engineering for total meniscal substitution: animal study in sheep model. Tissue Eng Part A **14**, 1067, 2008.
34. Tienen, T.G., Heijkants, R.G., Buma, P., De Groot, J.H., Pennings, A.J., and Veth, R.P. A porous polymer scaffold for meniscal lesion repair—a study in dogs. Biomaterials **24**, 2541, 2003.
35. Baker, B.M., and Mauck, R.L. The effect of nanofiber alignment on the maturation of engineered meniscus constructs. Biomaterials **28**, 1967, 2007.
36. De Groot, J.H., Zijlstra, F.M., Kuipers, H.W., *et al.* Meniscal tissue regeneration in porous 50/50 copoly (L-lactide/ε-caprolactone) implants. Biomaterials **18**, 613, 1997.
37. Mow, V.C., Kuei, S.C., Lai, W.M., and Armstrong, C.G. Biphasic creep and stress relaxation of articular cartilage in compression? Theory and experiments. J Biomech Eng **102**, 73, 1980.
38. McDevitt, C.A., and Webber, R.J. The ultrastructure and biochemistry of meniscal cartilage. Clin Orthop Relat Res **8,** 1990.
39. Melrose, J., Smith, S., Cake, M., Read, R., and Whitelock, J. Comparative spatial and temporal localisation of perlecan, aggrecan and type I, II and IV collagen in the ovine meniscus: an ageing study. Histochem Cell Biol **124**, 225, 2005.

Address correspondence to:
Michael G. Dunn, PhD
Department of Orthopaedic Surgery
Robert Wood Johnson Medical School
Rutgers Biomedical and Health Sciences
51 French St.
New Brunswick, NJ 08901

E-mail: dunnmg@rwjms.rutgers.edu

Received: June 1, 2018
Accepted: October 5, 2018
Online Publication Date: February 25, 2019

Downloaded by Univ Of Pennsylvania from www.liebertpub.com at 04/18/19. For personal use only.